3D MODELLING OF THE ERLP IR-FEL

D.J. Dunning, N.R. Thompson and J.A. Clarke, ASTeC, STFC Daresbury Laboratory, UK.
B.W.J. M^{c}Neil, SUPA, Department of Physics, University of Strathclyde, Glasgow, UK.

Abstract

The Energy Recovery Linac Prototype (ERLP) facility is currently being commissioned at Daresbury Laboratory. It serves as a testbed for technologies to be used in the proposed 4th Generation Light Source (4GLS) facility. As part of the ERLP facility, an infra-red oscillator FEL is due to be commissioned early in 2008. In this paper we present full three dimensional, time-dependent modelling of the ERLP IR-FEL using Genesis 1.3 in combination with a paraxial optical propagation code (OPC). We also discuss how this work will be used to inform commissioning of the FEL.

INTRODUCTION

The full details of the design for the ERLP IR-FEL are presented in [1] and summarised in Table 1 and a plan of the FEL is shown in Figure 1. Commissioning of the FEL is scheduled to begin early in 2008, and in preparation for this, full three dimensional modelling of the FEL has been carried out using Genesis 1.3 [2] in combination with a paraxial optical propagation code (OPC [3]). Both steady state and time-dependent simulations have been performed for three different modes of operation of the FEL. The results detailed in this paper will serve as a guide to the expected performance of the FEL during the commissioning period and will allow a comparison with experimental results so as to better inform FEL modelling for the 4GLS project.

Table 1: ERLP IR-FEL design parameters.

Parameter	Value
Wiggler period	0.027 m
Gap (fixed)	12 mm
Number of periods	40
Wiggler length	1.08 m
Deflection parameter, K	1.0
Nominal electron beam energy	35 MeV
Bunch charge	80 pC
Bunch length (rms)	<0.6 ps
Normalised emittance	10 mm-mrad
Energy spread (rms)	0.1 %
Optical cavity length	9.22438 m
Radiation wavelength (at 35 MeV beam energy)	4.394 µm

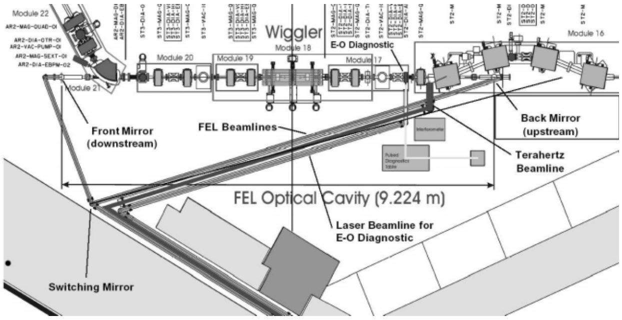

Figure 1: Plan of the FEL.

Operating Modes

The three proposed operating modes of the FEL are as follows: **normal mode**, **commissioning mode**, and **transmissive outcoupling mode**. A summary of the parameters for the different operating modes is given in Table 2. In transmissive outcoupling mode the electron bunch length is doubled, apart from this, the differences between different modes are in the mirror radii of curvature (ROC) and outcoupling method.

NORMAL MODE

The normal operating mode is designed to have maximum gain [4] and optimum output power. Details of this optimisation are included in the next section. The cavity is of a symmetric near-concentric design, of length D = 9.22438 m, with mirror ROC R = 4.75 m. The mirror angular alignment tolerance is $\ll$ 76 µrad. Outcoupling is via a 1.5 mm radius hole in the downstream mirror, giving a 12 % outcoupling fraction (chosen to maximise the output power).

The optical mode radius at the centre of the wiggler is w_0 = 1.04 mm. At this location the matched electron beam radii are σ_x = 0.24 mm and σ_y = 0.30 mm. The electron beam jitter (in transverse position) is expected to be no more than 10 % of the beam radius. This means that the jitter in electron beam position is no greater than 3 % of the optical mode size and ensures the coupling between electrons and radiation is near-optimal. The optical mode radius on the mirror surface, assuming the fundamental transverse mode TEM$_{00}$ is w_{mirror} = 6.15 mm compared to a mirror aperture radius of a = 19 mm. The ratio $a/w_m \approx$ 3:1: this is large enough to ensure that diffraction losses from the fundamental mode are minimal. All higher order transverse modes are wider, and will therefore suffer more diffraction loss - this is advantageous because it encourages lasing at the fundamental mode. In effect the limited mirror aperture acts as a crude method of transverse mode control.

Table 2: A summary of parameters for the different operating modes (the abbreviations “US” and “DS” refer to upstream and downstream respectively). The parameters: stability, angular alignment tolerance, mode size, cavity loss and single pass gain are calculated using standard design formulae.

Mode	**Normal**		**Commissioning**		**Transmissive**	
	US mirror	*DS mirror*	*US mirror*	*DS mirror*	*US mirror*	*DS mirror*
Mirror Material	Cu/Au	Cu/Au	Cu/Au	Cu/Au	Dielectric	Cu/Au
Reflectivity	>98%	>98%	>98%	>98%	3% trans.	>98%
ROC (m)	4.75	4.75	4.75	4.75	5.0	5.0
Mirror aperture radius (mm)	19	19	19	19	19	19
Hole radius (mm)	No hole	1.5	0.75	0.75	No hole	No hole
Outcoupling type (location)	Hole (DS)		Holes (DS + US)		Transmissive (US)	
Stability g^2	0.88		0.88		0.71	
Angular alignment tolerance θ_m (μrad)	$\ll$ 76		$\ll$ 76		$\ll$ 157	
Mode at waist w_0 (mm)	1.04		1.04		1.36	
Mode at mirror w_{mirror} (mm)	6.15		6.15		4.61	
Total cavity loss (%)	16		10		5	
Single pass gain (%)	72		72		25	
Electron bunch length σ_t (ps)	0.6		0.6		1.2	

Cavity optimisation

The cavity geometry has been varied around the proposed working point by changing the ROC of the mirrors simultaneously such that the waist position of the lowest order cold-cavity mode is kept constant. Figure 2 shows the effect of varying the radius of the outcoupling hole and the ROC of the cavity mirrors on the output power after 100 passes (by which time the FEL output is stable for almost all parameter sets used). This work has been carried out using Genesis 1.3 and OPC in steady-state mode. The results show that the proposed working point for normal mode operation (hole radius = 1.5 mm, mirror ROC = 4.75 m) is near optimum in terms of output power (~7.5 MW). The reduced output power around ROC = 4.8 m can be explained by considering the shape of the power profile at the downstream mirror (see Figure 4); the intensity cross-section peaks off-axis, hence the on-axis power outcoupled through the hole is lower.

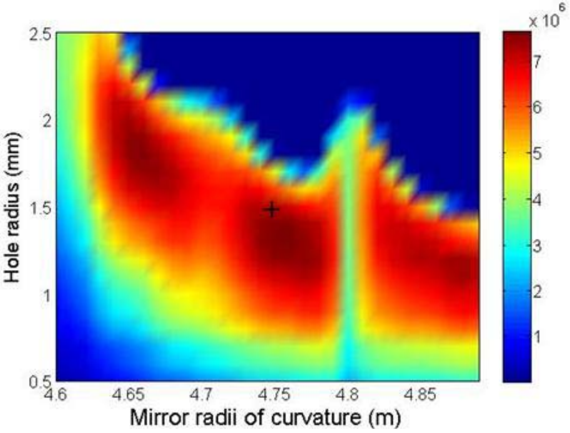

Figure 2: Output power (W) as a function of hole radius and mirror radii of curvature (i.e. keeping waist position constant). For normal operation, the hole radius is 1.5 mm and mirror ROC is 4.75 m.

For the proposed working point, the normalised intensity cross sections at saturation are shown in Figure 3 at different points within the optical cavity.

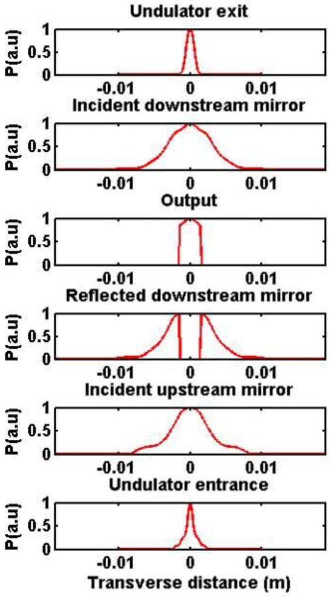

Figure 3: The normalised intensity cross sections at saturation, for different points within the optical cavity. Mirror radii of curvature = 4.75 m. The extent of the figure in the x-direction is equal to the mirror size (radius = 19 mm).

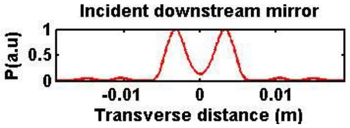

Figure 4: The normalised intensity cross section at the downstream mirror, at saturation, for mirror radii of curvature = 4.8 m.

Time-dependent simulations

Using Genesis 1.3 in time-dependent mode allows us to model the effects of cavity detuning, we are however, limited to detune the cavity only to half-integer multiples of the wavelength. Figure 5 show the cavity detuning curve for simulations of the FEL operating in normal mode. Higher peak output power (~16 MW at a cavity detuning of 2.2 µm) is seen compared to the steady state result (~7.5 MW).

Shown as a comparison is the corresponding cavity detuning curve for simulations performed using the one-dimensional code FELO [5]. There is a fairly good agreement between the two codes, particularly at smaller detuning values. Shown in Figure 6 is a comparison of the results from Genesis/OPC and FELO for a cavity detuning value of 4.4 µm (where the output power agreement between the two codes is closest); the longitudinal profile of the output radiation at saturation is plotted. There is a good agreement between the two codes for the longitudinal profiles of the FEL output at saturation.

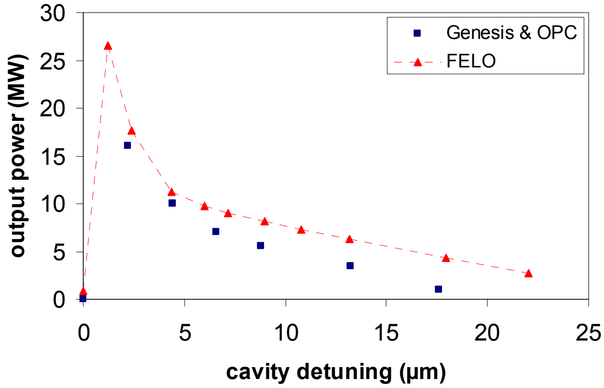

Figure 5: Output power at saturation against cavity detuning value for simulations of the FEL operating in normal mode, using Genesis 1.3/OPC and FELO.

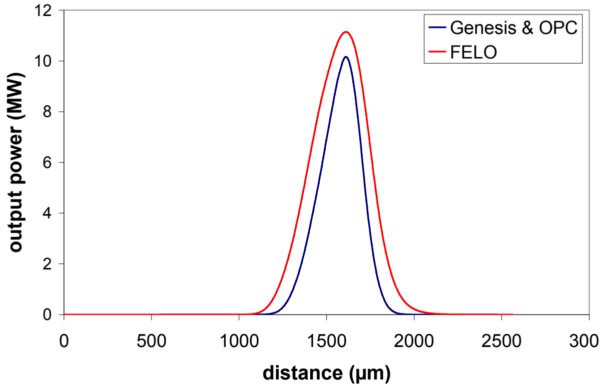

Figure 6: Longitudinal profile of the FEL output at saturation for a cavity detuning of 4.4 µm. Comparison between Genesis/OPC and FELO.

Shown in Figures 7 and 8 is the variation of longitudinal profile of the output radiation with cavity roundtrip number for two different cavity detuning values. Figure 7 shows the results with a cavity detuning of 2.2 µm; the width of the pulse is seen to be narrower than for the detuning value of 13.2 µm shown in Figure 8.

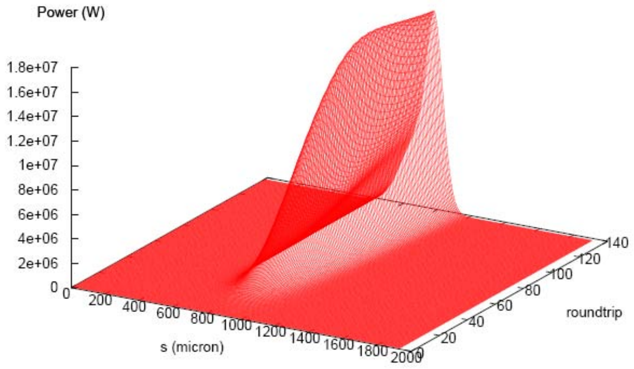

Figure 7: Variation of longitudinal profile of the output radiation with cavity roundtrip number for cavity detuning = 2.2 µm.

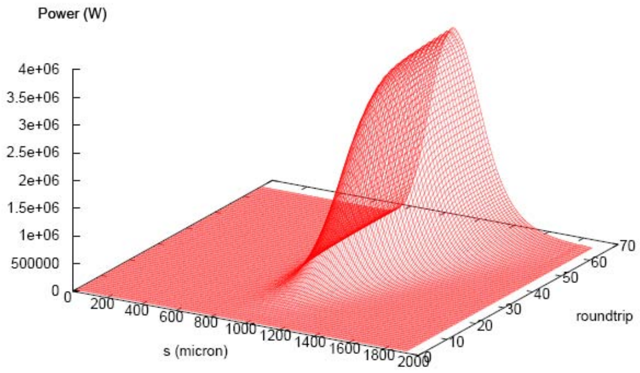

Figure 8: Variation of longitudinal profile of the output radiation with cavity roundtrip number for cavity detuning = 13.2 µm.

COMMISSIONING MODE

The commissioning mode of operation is designed for achieving first lasing; the cavity geometry is the same as for normal mode but outcoupling is via both mirrors. During commissioning we plan to monitor the FEL output directly at the upstream mirror while simultaneously monitoring the output from the downstream mirror in the diagnostics room. We therefore decouple the two problems of correctly steering the cavity to achieve lasing and correctly steering the output radiation down the beampipe to the diagnostics room.

Since outcoupling in this mode of operation is from both mirrors, smaller holes (0.75 mm radius) will be used, compared to the single hole used in normal mode operation. It is anticipated that this will reduce transverse mode distortion. Figure 9 shows the normalised intensity cross sections at saturation, at different points within the optical cavity. From the undulator entrance cross section it is evident that there is some higher order mode content in the radiation field.

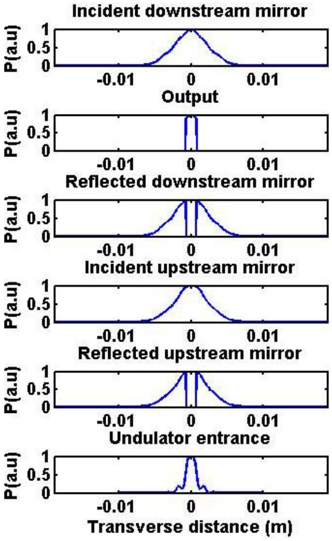

Figure 9: The normalised intensity cross sections at saturation for the FEL operating in commissioning mode, for different points within the optical cavity.

Time dependent simulations using Genesis 1.3 and OPC have been performed for the FEL operating in commissioning mode. Figure 10 shows the variation of output power with cavity detuning value. Figure 11 shows the variation of longitudinal profile of the output radiation from the downstream hole with cavity roundtrip number, for a cavity detuning of 2.2 μm.

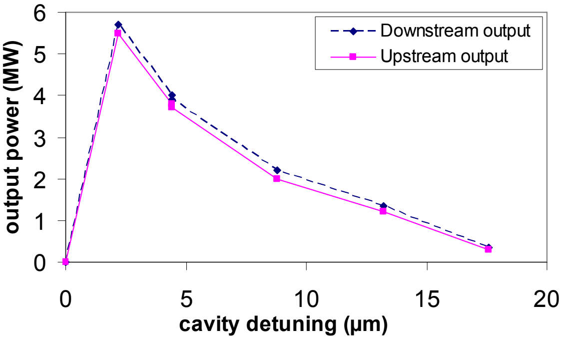

Figure 10: Output power at saturation against cavity detuning value for the simulations of the FEL operating in commissioning mode, using Genesis 1.3/OPC and FELO.

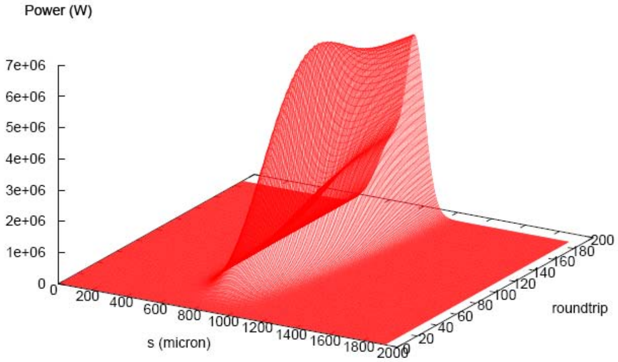

Figure 11: Variation of longitudinal profile of the output radiation from the downstream mirror with cavity roundtrip number for cavity detuning = 2.2 μm.

TRANSMISSIVE OUTCOUPLING MODE

The transmissive outcoupling mode of operation is designed to give us experience of using the transmissive outcoupling method and to increase the tolerances to electron beam transverse and longitudinal jitter and mirror angular alignment. The mirror cavity is designed to be further from concentric; increasing the mirror ROC to 5.0 m increases the optical waist to w_0 = 1.36 mm, reduces the cavity stability parameter g^2 to 0.71 and relaxes the angular alignment tolerance to $\ll$ 157 μrad. The electron bunch length is doubled to σ_t = 1.2 ps which halves the peak current but the calculated single pass gain is still 25 %, sufficient to lase easily with the outcoupling fraction reduced to 3 %.

The potential problem of mode distortion caused by hole outcoupling is removed by outcoupling using a partially transmitting (3 %) dielectric mirror. Because the cavity is further from concentric (compared to normal mode), the mode sizes shown in Figure 12 are wider at the waist and narrower at the mirrors compared to Figure 3. Time dependent simulations using Genesis 1.3 and OPC have been performed for the FEL operating in this mode and output powers of up to 12 MW are seen.

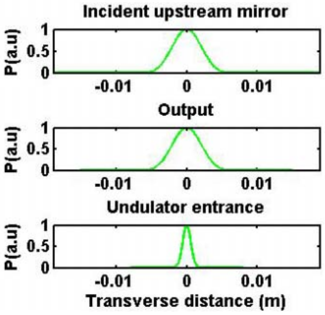

Figure 12: The normalised intensity cross sections at saturation for the FEL in transmissive outcoupling mode, at different points within the optical cavity.

CONCLUSION

Full three dimensional modelling of the ERLP IR-FEL has been carried out for the three different modes of operation of the FEL. For normal mode operation, the proposed cavity geometry and outcoupling hole radius have been shown to be near optimum in terms of output power. Time dependent simulations indicate a peak output power of ~16 MW at a cavity detuning of 2.2 μm.

REFERENCES

[1] N. Thompson, ERL Prototype FEL, internal report, *erlp-ofel-rpt-0001*, 2003.

[2] S. Reiche, Nucl. Inst. Meth. Phys. Res. A, 429, 243, (1999).

[3] J. G. Karssenberg et al, FEL-Oscillator Simulations with Genesis 1.3, FEL Conf 2006, 407.

[4] N. Thompson, ERL Prototype FEL: Electron Beam Matching, internal report, *erlp-ofel-rpt-0006*, 2004.

[5] B.W.J. McNeil et al, FELO, a one dimensional time dependent FEL oscillator code, FEL Conf. 2006, 59.